New Approach for Estimating the Input Fault Based on the Sliding Window Identification Technique of the SISO ARX-Laguerre Multimodel

Hajer BENAMOR[1]*, Marwa YOUSFI[1], Larbi CHRIFI ALAOUI[2], Hassani MESSAOUD[1]

[1] Laboratory of Automatic, Signal and Image Processing, Department of Electrical Engineering, School of Engineers Monastir-Tunisia, Ibn El Jazzar 5019 Monastir, Tunisia
hageramor@gmail.com (**Corresponding author*), yousfimarwa90@gmail.com, assani.messaoud@enim.rnu.tn

[2] Laboratory of Innovative Technology (LTI-UR-UPJV 3899) University of Picardie Jules Verne, 80000 Amiens, France
larbi.alaoui@u-picardie.fr

Abstract: This article focuses on developing a new approach for diagnosing of nonlinear systems. This approach consists in estimating the input fault by using the proposed ARX-Laguerre multimodel (Adaily, 2018) in its decoupled structure. This method is processed in two consecutive steps. The first consists in the offline identification of parameters of the ARX-Laguerre multimodel (weighting functions, Laguerre poles and -Fourier coefficients). The second step proposes an input fault estimation algorithm based on the online update of the parameters using the sliding window principle. This proposed diagnosis approach is implemented on a Continuously Stirred Reactor (CSTR) Benchmark to estimate the input fault. A comparative study regarding the results provided by a Proportional Integral (PI) observer based on the decoupled ARX-Laguerre multimodel is performed to attest this new approach.

Keywords: Multimodel, ARX Laguerre, Genetic Algorithm, Parameter optimisation, Sliding window, Input fault estimation, PI observer.

1. Introduction

In order to develop diagnosis or control strategies of a nonlinear system one has to provide a model for such a system. Several modeling approaches have been developed in the specialized literature such as: NARX, NARMAX, Volterra series (Fang et al., 2022; Levin et al.; Nguyen & Yin, 2017; Wang, 2020; Wang et al., 2022), structured block models (Wiener and Hammerstien) (Brouri et al., 2022; Mzyk & Wachel, 2017; Quachio & Garcia, 2019) and multimodels (Wang, 2020; Young & Holsteen, 2017). The latter approach, which will be used in this paper, consist in representing a nonlinear system by a finite number of submodels. These linear submodels describe the dynamic behavior of the system for each fraction of the operating domain. In the specialized literature, two multimodel structures have been developed: the coupled multimodel (Takagi & Sugeno, 1985), in which the submodels share the same state vector and the decoupled multimodel (Shin et al., 2020), in which each submodel has its own state vector. Since each submodel can be decomposed on the Laguerre orthogonal basis, nonlinear systems can be represented as a linear with respect to the Fourier coefficients characterizing this decomposition which allows the application of classical identification procedures.

In this context, nonlinear systems modeling using decoupled ARX-Laguerre can be mentioned. In (Adaily et al., 2018), the authors have exploited multimodel approach with the ARX-Laguerre model. For this representation, each submodel was express by an ARX-Laguerre linear model. The synthesis of the decoupled ARX-Laguerre multimodel requires firstly the estimation of the ARX-Laguerre multimodel parameters using a recursive identification method, then the determination of the parameters of the weighting functions. These latter will be identified using Genetic Algorithms (GA).

For the diagnosis of complex nonlinear systems, Takagi–Sugeno (T–S) fuzzy models provides a solution to the actuator fault estimation problem estimation problem, which consists in a set of locally linearized dynamics connected by fuzzy membership functions (Han et al., 2023; Zhang et al., 2023). However, the reconstructed T-S fuzzy model may contain a large number of fuzzy local models for the nonlinear system with complicated nonlinearities (Li et al., 2023). To avoid this problem, this paper proposes also a new method for estimating the input fault or the actuator fault based on the ARX-Laguerre multimodel which is characterized by

https://doi.org/10.24846/v32i4y202311

a simple recursive vector representation and a significant parametric reduction. This can also be achieved by exploiting the online parametric identification approach over a sliding window recently addressed in (Adaily et al., 2018), for the detection of the operating mode change. Based on the same principle, the new proposed approach of input fault estimation consists in updating parameters according to the evolution of the output of the system, influenced by the input impact with or without the presence of the fault. Thus, the online identification of the parameters relies on updating the Fourier coefficients, as well as the Laguerre poles, by shifting the sliding window at each sampling time, while keeping the weighting functions identified by genetic algorithms. This update can be obtained by implementing the offline parametric identification method on a sliding window of variable size. Following this update, the development of an algorithm is proposed to estimate the input fault at each sampling time.

To validate the offline identification method of the ARX-Laguerre multimodels parameters, as well as this new approach of input fault estimation they were applied to a CSTR Benchmark. To prove the efficiency of the method proposed for input fault estimation in this paper, a comparative study with input fault estimation using the classical PI observer based on the ARX-Laguerre multimodel (Benamor et al., 2020) is presented.

Accordingly, the contributions of this paper are mainly threefold: first, the proposition of an algorithm for the optimization of the ARX-Laguerre multimodel using genetic algorithm; second, the development of a new algorithm for nonlinear systems diagnosis according to the input fault estimation applied on the proposed ARX-Laguerre multimodel based on the online parameters update using the sliding window principle; and third, the validation of the proposed algorithm for parametric identification and input fault estimation through a comparative study regarding the results provided by a Proportional Integral (PI) observer.

The present paper is organized as follows. Section 2 focuses on a bibliographical study of the simple recursive representation of decoupled ARX-Laguerre multimodel. In section 3, an algorithm for the offline parametric optimization of the ARX-Laguerre multimodel based on Genetic Algorithms is developed. In section 4, the algorithm of the new approach needed for estimating the input fault is developed. Section 5 is allocated to the validation of two algorithms developed on a CSTR Benchmark and to a comparative study with an input fault estimation method based on the PI observer. Finally, section 6 provides the conclusion of the proposed research.

2. Decoupled ARX-Laguerre Multimodel

Following the development of Bouzrara et al. (2013), the decoupled ARX-Laguerre of a sub-model (s) is:

$$\begin{cases} \boldsymbol{X}^s(k+1) = \boldsymbol{A}^s\, \boldsymbol{X}^s(k) + \boldsymbol{b}_u^s\, u(k) + \boldsymbol{b}_y^s\, y^s(k) \\ y^s(k) = (\boldsymbol{C}^s)^T\, \boldsymbol{X}^s(k) \end{cases} \quad (1)$$

where $u(k)$ is the input, s = 1,..., L and L is the number of submodels.

$y^S(k)$ is the submodel output given by:

$$y^s(k) = \sum_{n=0}^{n_a-1} g_{n,a}^s\, x_{n,y}^s(k) + \sum_{n=0}^{n_b-1} g_{n,b}^s\, x_{n,u}^s(k) \quad (2)$$

where n_a and n_b are the truncating orders of the ARX-Laguerre submodel, $g_{n,a}^s$ and $g_{n,b}^s$ are the Fourier coefficients characterizing the sth ARX-Laguerre submodel and $x_{n,y}^s$ and $x_{n,u}^s$ are the filtered outputs and the filtered inputs respectively, which are the components of the vector $\boldsymbol{X}^s(k)$ as:

$$\begin{aligned} \boldsymbol{X}^s(k) = \Big[& x_{0,y}^s(k), \ldots, x_{n_a-1,y}^s(k), \\ & x_{0,u}^s(k), \ldots, x_{n_b-1,u}^s(k) \Big]^T \in \Re^{(n_a+n_b)} \end{aligned} \quad (3)$$

- $\boldsymbol{A}^s$ is a square matrix depending on the Laguerre poles ξ_a^s and ξ_b^s:

$$\boldsymbol{A}^s = \begin{pmatrix} \boldsymbol{A}_y^s & 0_{n_a,n_b} \\ 0_{n_b,n_a} & \boldsymbol{A}_u^s \end{pmatrix} \in \Re^{n_a+n_b} \quad (4)$$

where $0_{q,m}$ is the null matrix $(q \times m)$ dimensional.

$\boldsymbol{A}_y^s$ and $\boldsymbol{A}_u^s$ are square matrices given by:

$$\boldsymbol{A}_y^s = \begin{pmatrix} \xi_a^s & 0 & \cdots & 0 \\ 1-(\xi_a^s)^2 & \xi_a^s & \cdots & 0 \\ -\xi_a^s(1-(\xi_a^s)^2) & \xi_a^s & \cdots & 0 \\ \vdots & \vdots & \ddots & \vdots \\ (-\xi_a^s)^{n_a-2}(1-(\xi_a^s)^2) & (-\xi_a^s)^{n_a-3}(1-(\xi_a^s)^2) & \cdots & \xi_a^s \end{pmatrix} \in \Re^{n_a} \quad (5)$$

$$\boldsymbol{A}_u^s = \begin{pmatrix} \xi_b^s & 0 & \cdots & 0 \\ 1-(\xi_b^s)^2 & \xi_b^s & \cdots & 0 \\ -\xi_b^s(1-(\xi_b^s)^2) & \xi_b^s & \cdots & 0 \\ \vdots & \vdots & \ddots & \vdots \\ (-\xi_b^s)^{n_b-2}(1-(\xi_b^s)^2) & (-\xi_b^s)^{n_b-3}(1-(\xi_b^s)^2) & \cdots & \xi_b^s \end{pmatrix} \in \Re^{n_b} \quad (6)$$

- b_u^s and b_y^s are column vectors of dimensions $(n_a + n_b)$ depending on the Laguerre pole:

$$\boldsymbol{b}_y^s = \sqrt{1-(\xi_a^s)^2} \begin{bmatrix} 1 \\ -\xi_a^s \\ \left(-\xi_a^s\right)^2 \\ \vdots \\ \left(-\xi_a^s\right)^{n_a-1} \\ 0_{n_b,1} \end{bmatrix} \in \Re^{(n_a+n_b)}$$

$$\boldsymbol{b}_u^s = \sqrt{1-(\xi_b^s)^2} \begin{bmatrix} 0_{n_a,1} \\ 1 \\ -\xi_b^s \\ \left(-\xi_b^s\right)^2 \\ \vdots \\ \left(-\xi_b^s\right)^{n_b-1} \end{bmatrix} \in \Re^{(n_a+n_b)} \quad (7)$$

- $\boldsymbol{C}^s$ is a column vector arranging the Fourier coefficients:

$$\boldsymbol{C}^s = \left[g_{0,a}^s, \ldots, g_{n_a-1,a}^s, g_{0,b}^s, \ldots, g_{n_b-1,b}^s \right]^T \in \Re^{(n_a+n_b)} \quad (8)$$

Figure 1 presents the architecture of the decoupled ARX-Laguerre multimodel.

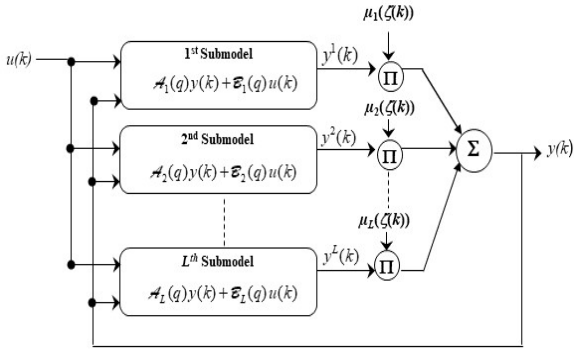

Figure 1. Decoupled ARX-Laguerre multimodel structure

where $y(k)$ is the output of the ARX-Laguerre multimodel given by the following expression:

$$y(k) = \sum_{s=1}^{L} \mu_s(\zeta(k))\, y^s(k) \quad (9)$$

and $\mu_s(\zeta(k))$ is a weighting function characterizing the contribution of each ARX Laguerre submodel;

with $\zeta(k)$ being a decision parameter which can be chosen as either input or output of the system.

These functions satisfy the convex property:

$$\sum_{s=1}^{L} \mu_s(\zeta(k)) = 1 \text{ and } 0 \le \mu_s(\zeta(k)) \le 1; \ \forall s = 1 \ldots L \quad (10)$$

These functions $\mu_s(\zeta(k))$ can be built based on Gaussian functions $\omega_s(\zeta(k))$:

$$\mu_s(\zeta(k)) = \frac{\omega_s(\zeta(k))}{\sum_{j=1}^{L} \omega_j(\zeta(k))} \quad (11)$$

with

$$\omega_s(\zeta(k)) = \exp\left(-\frac{\left(\zeta(k) - c_s\right)^2}{\sigma_s^2} \right) \quad (12)$$

where c_s is the center of $\omega_s(\zeta(k))$ and σ_s represents its standard deviation.

3. Offline Parametric Identification

3.1 Fourier Coefficients Identification

The compact recursive vector representation of the ARX-Laguerre multimodel is obtained from equations (1) and (9).

$$\begin{cases} \underline{\boldsymbol{X}}(k+1) = (\underline{\boldsymbol{A}} + \underline{\boldsymbol{b}}_c)\underline{\boldsymbol{X}}(k) + \underline{\boldsymbol{b}}_u u(k) \\ y(k) = \underline{\boldsymbol{C}}^T \boldsymbol{M}_\mu \underline{\boldsymbol{X}}(k) \end{cases} \quad (13)$$

- $\underline{\boldsymbol{X}}(k)$ is the column vector given by:

$$\underline{\boldsymbol{X}}(k) = \left[\left[\boldsymbol{X}^1(k) \right]^T, \ldots, \left[\boldsymbol{X}^L(k) \right]^T \right]^T \in \Re^{L(n_a+n_b)} \quad (14)$$

and $\underline{\boldsymbol{A}}$ is a square matrix

$$\underline{\boldsymbol{A}} = \begin{pmatrix} \boldsymbol{A}^1 & 0_{n_a+n_b} & \cdots & 0_{n_a+n_b} \\ 0_{n_a+n_b} & \boldsymbol{A}^2 & \ddots & \vdots \\ \vdots & \ddots & \ddots & 0_{n_a+n_b} \\ 0_{n_a+n_b} & \cdots & 0_{n_a+n_b} & \boldsymbol{A}^L \end{pmatrix} \in \Re^{L(n_a+n_b)} \quad (15)$$

- $\underline{\boldsymbol{C}}, \underline{\boldsymbol{b}}_c$ and $\underline{\boldsymbol{b}}_u$ are $L(n_a + n_b)$ dimensional column vectors defined by:

$$\underline{\boldsymbol{C}} = \left[(\boldsymbol{C}^1)^T, \ldots, (\boldsymbol{C}^L)^T \right]^T ; \ \underline{\boldsymbol{b}}_u = \left[\left(\boldsymbol{b}_u^1\right)^T \ldots \left(\boldsymbol{b}_u^L\right)^T \right]^T ;$$
$$\underline{\boldsymbol{b}}_C = bloc\, diag \left[\left(\boldsymbol{b}_y^1\right)^T \times (\boldsymbol{C}^1)^T, \ldots, \left(\boldsymbol{b}_y^L\right)^T \times (\boldsymbol{C}^L)^T \right]^T \quad (16)$$

- $\boldsymbol{M}_u$ is a $L(n_a+n_b)$ dimensional square matrix defined by:

$$\boldsymbol{M}_{\mu}=\begin{pmatrix}\mu_1 \boldsymbol{I}_{n_a+n_b} & 0_{n_a+n_b} & \cdots & 0_{n_a+n_b}\\ 0_{n_a+n_b} & \mu_2 \boldsymbol{I}_{n_a+n_b} & \ddots & \vdots\\ \vdots & \ddots & \ddots & 0_{n_a+n_b}\\ 0_{n_a+n_b} & \cdots & 0_{n_a+n_b} & \mu_L \boldsymbol{I}_{n_a+n_b}\end{pmatrix} \quad (17)$$

Referred to (13), the recursive identification of the vector $\boldsymbol{C}^s$ is based on minimizing the regularized quadratic error J at each iteration p (Fang et al., 2022):

$$J(p)=\sum_{k=1}^{p}\left(y_m(k)-\underline{\boldsymbol{C}}^T\boldsymbol{M}_{\mu}\underline{\boldsymbol{X}}(k)\right)^2 +\alpha\sum_{s=1}^{L}\left(\sum_{n=0}^{n_a-1}\left[g_{n,a}^s(p-1)-g_{n,a}^s(p)\right]^2+\sum_{n=0}^{n_b-1}\left[g_{n,b}^s(p-1)-g_{n,b}^s(p)\right]^2\right) \quad (18)$$

where $\alpha > 0$ is a regularization constant which can keep a low variation of the Fourier coefficients between two consecutive instants.

From (18), the matrix form of J can be rewritten as:

$$J(p)=\left[Y_m(p)-\underline{\psi}(p)\underline{C}(p)\right]^T\left[Y_m(p)-\underline{\psi}(p)\underline{C}(p)\right] +\alpha\left[\underline{C}(p-1)-\underline{C}(p)\right]^T\left[\underline{C}(p-1)-\underline{C}(p)\right] \quad (19)$$

where

$$Y_m(p)=\left[y_m(1),.....,y_m(p)\right]^T;\ Y(p)=\left[y(1),.....,y(p)\right]^T=\underline{\psi}(p)\underline{C}(p) \quad (20)$$

$$\underline{\psi}(p)=\left[\psi(1).....\psi(p)\right]^T\in\Re^{p\times L(n_a+n_b)};\ \psi(p)=M_{\mu}X(p)\in\Re^{L(n_a+n_b)} \quad (21)$$

$$\underline{C}(p)=\left[\left[c^1(p)\right]^T,.....,\left[c^L(p)\right]^T\right]^T \text{ where}$$

$$c^s(p)=\left[\ g_{0,a}^s(p),\ldots,g_{n_a-1,a}^s(p),g_{0,b}^s(p),\ldots,g_{n_b-1,b}^s(p)\ \right]^T \quad (22)$$

The estimated vector of Fourier coefficients $\hat{\underline{C}}(p)$ is:

$$\hat{\underline{C}}(p)=\left(\underline{\psi}^T(p)\underline{\psi}(p)+\alpha\boldsymbol{I}_{L(n_a+n_b)}\right)^{-1}\times\left(\underline{\psi}^T(p)Y_m(p)+\alpha\,\hat{\underline{C}}(p-1)\right) \quad (23)$$

where $\boldsymbol{I}_{L(n_a+n_b)}$ is a $L(n_a+n_b)$ dimensional identity matrix.

3.2 Laguerre Poles Identification

One of the advantages of the ARX Laguerre multimodel is the reduction of the number of parameters when the Laguerre poles reach their optimal values. To achieve this, the Laguerre poles are calculated in an iterative way, according to the Fourier coefficients of the ARX-Laguerre multimodel (Han et al., 2023). Therefore, the following quantities are defined:

$$T_{1,a}^s=\sum_{n=0}^{\infty}(2n+1)\left(g_{n,a}^s\right)^2;\quad T_{1,b}^s=\sum_{n=0}^{\infty}(2n+1)\left(g_{n,b}^s\right)^2 \quad (24)$$

$$T_{2,a}^s=2\sum_{n=0}^{\infty}n\ g_{n,a}^s\ g_{n-1,a}^s;\quad T_{2,b}^s=2\sum_{n=0}^{\infty}n\,g_{n,b}^s\,g_{n-1,b}^s \quad (25)$$

Hence, the optimal Laguerre poles $\xi_{opt,a}^s$ and $\xi_{opt,b}^s$, $s=1,\ldots.L$ are obtained (Han et al., 2023):

$$\xi_{opt,i}^s=\begin{cases}\rho_i^s-\sqrt{\left(\rho_i^s\right)^2-1} & \text{if } \rho_i^s>1\\ \rho_i^s+\sqrt{\left(\rho_i^s\right)^2-1} & \text{if } \rho_i^s<-1\end{cases},\ s=1,\ldots,L,\ i=a,b \quad (26)$$

where

$$\rho_i^s=\frac{(1+(\xi_i^s)^2)\ T_{1,i}^s+2\ \xi_i^s\ T_{2,i}^s}{(1+(\xi_i^s)^2)\ T_{2,i}^s+2\ \xi_i^s\ T_{1,i}^s},\ s=1,\ldots,L,\ i=a,b \quad (27)$$

3.3 Identification of the Parameters of the Weighting Function Using Genetic Algorithms

Genetic Algorithms are based on the selection of the most suitable individuals from an initial population of random N_{ind} individuals. Using the genetic algorithm, a new population is produced following the application of three genetic operations: selection, crossing and mutation (Vajda et al., 2008). In the present case, the exploitation of Genetic Algorithms for the identification of weighting function is proposed. The optimal solution is obtained from the minimization of a *NMSE* (Normalized Mean Square Error) given by:

$$NMSE=\frac{\sum_{k=1}^{M}(y_m(k)-y(k))^2}{\sum_{k=1}^{M}(y_m(k))^2} \quad (28)$$

where M is the number of measurements.

A random initial population Ind of N_{ind} individuals of the parameters of the weighting functions is generated.

$$Ind=\left[\boldsymbol{c}^l,\boldsymbol{\sigma}^l\right]\in\Re^{1\times 2L};\quad l=1,...,N_{ind} \quad (29)$$

where:

- $\boldsymbol{C}^l$ is the vector containing the centers of the weighting functions:

$$\boldsymbol{c}^l=\left[c_1^l,...,c_L^l\right]\in\Re^{1\times L};\quad l=1,...,N_{ind} \quad (30)$$

- $\boldsymbol{\sigma}^l$ is the vector containing the dispersions:

$$\boldsymbol{\sigma}^l=\left[\sigma_1^l,...,\sigma_L^l\right]\in\Re^{1\times L};\quad l=1,...,N_{ind} \quad (31)$$

It can be noted that a number of iterations G_{max} of the genetic algorithm is fixed and that at each iteration the evaluation function *NMSE* is applied for the current population *Ind*. This evaluation

allows the selection of the best individuals resulting from the genetic operations of selection, crossover and mutation. These operations are applied at each iteration of the genetic algorithm until the parameters of the weighting functions converge to their optimal values. It should be noted that the evaluation of the *NMSE* criterion requires the calculation of the Laguerre poles and the Fourier coefficients.

Algorithm 1. Identification of the parameters of the weighting function with genetic algorithm

1. Assuming that there are M input/output data pairs $(u(k), y_m(k))$.
2. Fix the submodel number L, the truncating orders n_a and n_b and the regularization constant α.
3. Fix the iteration number G_{max}, the population size N_{ind}, as well as the crossover rate P_c (≤100%) and the mutation rate P_m (≤100%).
4. Initialization: Create a random initial population Ind of N_{ind} vectors of weighting functions parameters $Ind^l = [c^l, \sigma^l]$ and a set counter = 1.
5. As long as counter < G_{max}, for each population, do:
   5.1. Evaluation:
   a. Identify the Fourier coefficients and the Laguerre poles as follows:
   i. Estimate the Fourier coefficients $g_{n,a}^s$ and $g_{n,b}^s$ by (23) $\forall k = 1,\ldots,M$ knowing that $\underline{C}(0) = 0_{n_a+n_b,1}$.
   ii. Calculate $T_{1,i}^s$ and $T_{2,i}^s$, $i = a, b, s = 1, \ldots, L$ from (24) and (25) respectively.
   iii. If $T_{1,i}^s$ and $T_{2,i}^s$ are close to zero go to step b. Otherwise:
   - Calculate ρ_a^s and ρ_b^s from (27).
   - Update the poles $\xi_{opt,a}^s$ and $\xi_{opt,b}^s$ given in (26), then return to step (i).
   b. Evaluate the *NMSE* from (28).
   5.2. Selection: select $Pc \times N_{ind}$ individual of the up-to-date population depending on the evaluation of the values of the *NMSE*.
   5.3. Crossover and mutation: practice the crossover on the selected populations and then apply the mutation with a rate of P_m to generate the new population.
   5.4. Reintegration: The best new solution is inserted in the new population in ascending order according to its *NMSE* evaluation.
   5.5. increment the counter and back in step 5

4. Proposed Approach for the Input Fault Estimation

In what follows, the concept of the new proposed approach for estimating an input fault $\eta(k)$, injected at the system input $u(k)$, is presented. To achieve this, it is taken into consideration that, in the presence of the fault, the input is written in this additive form $u(k) + \eta(k)$ and, referring to (13), the output $y_\eta(k)$ with input fault is obtained as follows:

$$\begin{cases} \underline{X}(k+1) = (\underline{\boldsymbol{A}} + \underline{\boldsymbol{b}}_c)\underline{\boldsymbol{X}}(k) + \underline{\boldsymbol{b}}_u \left(u(k) + \eta(k)\right) \\ y_\eta(k) = \underline{\boldsymbol{C}}^T \boldsymbol{M}_\mu \underline{X}(k) \end{cases} \quad (32)$$

From (32), one obtains:

$$y_\eta(k) = \underline{\boldsymbol{C}}^T \boldsymbol{M}_\mu \left[(\underline{\boldsymbol{A}} + \underline{\boldsymbol{b}}_c)\underline{X}(k-1) + \underline{\boldsymbol{b}}_u u(k-1)\right] + \underline{\boldsymbol{C}}^T \boldsymbol{M}_\mu \underline{\boldsymbol{b}}_u \eta(k-1) \quad (33)$$

Thus, it can be noticed that the input fault $\eta(k)$ is retained in an additive form to the input $u(k)$ and that the quantities $\underline{\boldsymbol{A}}, \underline{\boldsymbol{b}}_c, \underline{\boldsymbol{b}}_u$ and $\underline{\boldsymbol{C}}$ remain unchanged. However, the output changes in presence of the fault which requires a new formulation of (32) as: $y_\eta(k) \neq y(k)$. In this case, an update of the quantities $\underline{\boldsymbol{A}}, \underline{\boldsymbol{b}}_c, \underline{\boldsymbol{b}}_u$ and $\underline{\boldsymbol{C}}$ is necessary. This update leads to a new identification of the parameters (Fourier coefficients and Laguerre poles) of the ARX Laguerre multimodel, in the presence of the input fault $\eta(k)$:

$$\begin{cases} \underline{\boldsymbol{X}}_\eta(k+1) = (\underline{\boldsymbol{A}}_\eta + \underline{\boldsymbol{b}}_{c,\eta})\underline{\boldsymbol{X}}_\eta(k) + \underline{\boldsymbol{b}}_{u,\eta}\, u(k) \\ y_\eta(k) = \underline{\boldsymbol{C}}_\eta^T \boldsymbol{M}_\mu \underline{\boldsymbol{X}}_\eta(k) \end{cases} \quad (34)$$

where:

- $\boldsymbol{A}_\eta$ is a square matrix of dimension $L(n_a + n_b)$ defined as follows:

$$\underline{\boldsymbol{A}}_\eta = \begin{pmatrix} \boldsymbol{A}_\eta^1 & 0_{n_a+n_b} & \cdots & 0_{n_a+n_b} \\ 0_{n_a+n_b} & \boldsymbol{A}_\eta^2 & \ddots & \vdots \\ \vdots & \ddots & \ddots & 0_{n_a+n_b} \\ 0_{n_a+n_b} & \cdots & 0_{n_a+n_b} & \boldsymbol{A}_\eta^L \end{pmatrix} \in \Re^{L(n_a+n_b)} \quad (35)$$

where $\boldsymbol{A}_\eta^s, s = 1,\ldots,L$ are matrices defined from (4), by replacing ξ_a^s and ξ_b^s with their updated values $\xi_{a,\eta}^s$ and $\xi_{b,\eta}^s$, respectively.

- $\underline{\boldsymbol{b}}_{c,\eta}$, $\underline{\boldsymbol{b}}_{u,\eta}$ and $\underline{\boldsymbol{C}}_\eta$ are column vectors defined as follows:

$$\underline{\boldsymbol{b}}_{c,\eta} = bloc\ diag\left[\left(\boldsymbol{b}_{y,\eta}^1\right)^T \times (\boldsymbol{C}_\eta^1)^T, \ldots, \left(\boldsymbol{b}_{y,\eta}^L\right)^T \times (\boldsymbol{C}_\eta^L)^T\right]^T \in \Re^{L(n_a+n_b)} \quad (36)$$

$$\underline{\boldsymbol{b}}_{u,\eta} = \left[\left[\boldsymbol{b}_{u,\eta}^1\right]^T, \ldots, \left[\boldsymbol{b}_{u,\eta}^L\right]^T\right]^T \in \Re^{L(n_a+n_b)} \quad (37)$$

$$\underline{\boldsymbol{C}}_\eta = \left[\left(\boldsymbol{C}_\eta^1\right)^T, \ldots, \left(\boldsymbol{C}_\eta^L\right)^T\right]^T \in \Re^{L(n_a+n_b)} \quad (38)$$

where the vectors $\boldsymbol{b}_{y,\eta}^{s}, \boldsymbol{b}_{u,\eta}^{s}$ and $\boldsymbol{C}_{\eta}^{s}$, $s=1,...,L$ are obtained from (7) and (8) by replacing ξ_{a}^{s}, ξ_{b}^{s} with $\xi_{a,\eta}^{s}$, $\xi_{b,\eta}^{s}$ and $g_{n,a}^{s}$, $g_{n,b}^{s}$ with their new updates $g_{n,a,\eta}^{s}, g_{n,b,\eta}^{s}$, respectively.

- $\underline{\boldsymbol{X}}_{\eta}(k)$ is a column vector of dimension $L(n_a+n_b)$.

The new form (34) needs the identification of the ARX-Laguerre multimodel resulting from the fault introduction. The output of system can be expressed as follows:

$$y_{\eta}(k)=\underline{\boldsymbol{C}}_{\eta}^{T}\boldsymbol{M}_{\mu}\left[(\underline{\boldsymbol{A}}_{\eta}+\underline{\boldsymbol{b}}_{c,\eta})\,\underline{\boldsymbol{X}}_{\eta}(k-1)+\underline{\boldsymbol{b}}_{u,\eta}u(k-1)\right] \quad (39)$$

Replacing $y_{\eta}(k)$ in (33) by its expression in (39), the expression of the input fault $\eta(k-1)$ is given by:

$$\begin{aligned}\eta(k-1)=&(\underline{\boldsymbol{C}}^{T}\boldsymbol{M}_{\mu}\underline{\boldsymbol{b}}_{u})^{-1}\Big[\underline{\boldsymbol{C}}_{\eta}^{T}\boldsymbol{M}_{\mu}\left((\underline{\boldsymbol{A}}_{\eta}+\underline{\boldsymbol{b}}_{c,\eta})\,\underline{\boldsymbol{X}}_{\eta}(k-1)+\underline{\boldsymbol{b}}_{u,\eta}u(k-1)\right)\\&-\underline{\boldsymbol{C}}^{T}\boldsymbol{M}_{\mu}\left((\underline{\boldsymbol{A}}+\underline{\boldsymbol{b}}_{c})\underline{\boldsymbol{X}}(k-1)+\underline{\boldsymbol{b}}_{u}u(k-1)\right)\Big]\end{aligned} \quad (40)$$

In what follows, the calculated input fault $\eta_{cal}(k)$ at iteration *k* is taken into consideration, so that:

$$\eta_{cal}(k)=\eta(k-1) \quad (41)$$

It should be emphasized that, in order to obtain the updated values of the Fourier coefficients and Laguerre poles, one opts for the exploitation of online identification on a sliding window $[\,p+1-n_0\,,\,p\,], \forall\, p>n_0$, where n_0 is the width of the window (Quachion & Garcia, 2019).

However, the online parametric -identification of the ARX-Laguerre multimodel on the sliding window relies on the update of the Laguerre poles. Then, the updates of the Fourier coefficients rely on a number of iterations n_0, while keeping the weighting functions obtained by the genetic algorithm. This update is obtained by implementing the offline parametric identification method on a sliding window. At each iteration $p>n_0$ in the interval $[\,p+1-n_0\,,\,p\,]$, the Fourier coefficient identification method is applied on the sliding window of n_0 observations which leads to the update of the Laguerre poles given by (26). The regularized criterion *J(p)* is written according to (18) in the following form:

$$\begin{aligned}J(p)=&\sum_{k=p+1-n_0}^{p}\left(y_m(k)-\underline{\boldsymbol{C}}_{\eta}^{T}\psi(k)\right)^{2}\\&+\alpha\sum_{s=1}^{L}\left(\sum_{n=0}^{n_a-1}\left[g_{n,a,\eta}^{s}(p-1)-g_{n,a,\eta}^{s}(p)\right]^{2}+\sum_{n=0}^{n_b-1}\left[g_{n,b,\eta}^{s}(p-1)-g_{n,b,\eta}^{s}(p)\right]^{2}\right)\end{aligned} \quad (42)$$

Subsequently, the estimated vector of Fourier coefficients is expressed as follows:

$$\hat{\underline{C}}_{\eta}(p)=\left(\underline{\psi}_{p,n_0}^{T}(p)\,\underline{\psi}_{p,n_0}(p)+\alpha I\right)^{-1}\left(\underline{\psi}_{p,n_0}^{T}(p)Y_{p,n_0}(p)+\alpha\,\hat{\underline{C}}_{\eta}(p-1)\right),\ \forall\, p>n_0 \quad (43)$$

with

$$\underline{\psi}_{p,n_o}=\left[\psi(p+1-n_0)\ldots\psi(p)\right]^{T}=\begin{pmatrix}\underline{\psi}_{p-1,n_0}\\ \psi^{T}(p)\end{pmatrix} \quad (44)$$

$$Y_{p,n_0}=\left[y_m(p+1-n_0),\ldots,y_m(p)\right]^{T}=\begin{pmatrix}Y_{p-1,n_0}\\ y_m(p)\end{pmatrix} \quad (45)$$

In order to check the execution of the update of the Laguerre poles depending on the estimated vector of Fourier coefficients $\hat{\underline{C}}_{\eta}(p)$, the following convergence criterion is taken into consideration:

$$\left\|\hat{\underline{C}}_{\eta}(p)-\hat{\underline{C}}_{\eta}(p-1)\right\|^{2}<\varepsilon \quad (46)$$

where ε is the convergence threshold.

At each iteration *k*, the vector of Fourier coefficients $\hat{\underline{C}}\,(p)$ is adapted on the sliding window $[\,p+1-n_0\,,\,p\,]$. A new estimation of the Laguerre poles is executed once the condition (46) isn't satisfied. The proposed input fault estimation algorithm is:

Algorithm 2. Input fault estimation algorithm

(1) Offline identification phase using algorithm For k=1,…,n_0, it is considered that $\eta_{cal}(k)=0$, $\hat{\underline{C}}_{\eta}(p)=\hat{\underline{C}}(H)$, $\xi_{a,\eta}^{s}=\xi$, $\xi_{b,\eta}^{s}=\xi_{b,\eta}^{s}$, $\forall\ s=1,...L$ and $y_{\eta}(k)=y(k)$ by applying (13).

(2) Online identification phase $\forall\ p>n_0$: for each iteration k of the interval [p+1−n_o , p]:

- 2.1. Measure the system output of y_m(k).
- 2.2. Calculate the vector $\hat{\underline{C}}_{\eta}(p)$ using (23).
- 2.3. If $\left\|\hat{\underline{C}}_{\eta}(p)-\hat{\underline{C}}_{\eta}(p-1)\right\|^{2}<\varepsilon$ then Calculate the value of the input fault $\eta_{cal}(k)$ from (40), increment and return to step 2.1. Otherwise: Compute the new Laguerre poles $\xi_{a,\eta}^{s}$ and $\xi_{b,\eta}^{s}$, $s=1,..,L$ from (26).
- 2.4. Calculate the matrices $\underline{\boldsymbol{A}}_{\eta}, \underline{\boldsymbol{b}}_{c,\eta}$ and $\underline{\boldsymbol{b}}_{u,\eta}$ from (35), (36) and (37).
- 2.5. Calculate the new vector of Fourier coefficients $\hat{\underline{C}}_{\eta}(p)$ from (43).
- 2.6. Calculate the vectors $\underline{\boldsymbol{X}}(k)$ and $\underline{\boldsymbol{X}}_{\eta}(k)$ from (32) and (34) respectively.
- 2.7. Calculate the value of the input fault $\eta_{cal}(k)$ from (40).
- 2.8. Increment p and return to step 2.1.

The proposed approach for estimating the input fault using the ARX-Laguerre multimodel is illustrated by Figure 2.

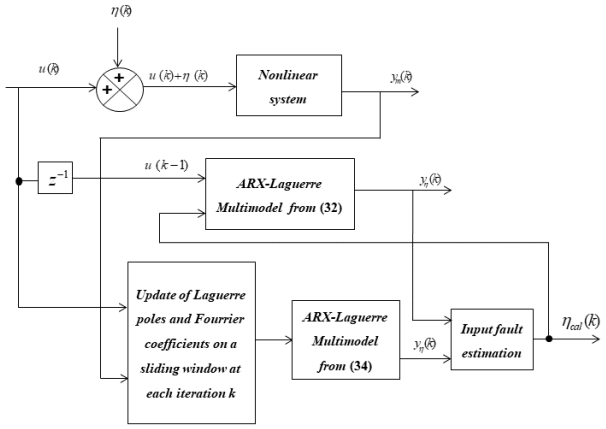

Figure 2. Proposed input fault estimation approach

5. Validation of the New Approach on the CSTR Benchmark

To test the performances of the developed algorithms, they are tested on CSTR (Seborg et al., 2004). First, Algorithm 1 is tested for the offline identification of parameters of the ARX-Laguerre multimodel. After that, Algorithm 2 is tested for input fault estimation, where both constant and random faults are considered. To highlight the performances of the new proposed approach, a comparative study with PI observer method based on the ARX-Laguerre multimodel is taken into consideration (Benamor et al., 2020).

The CSTR Benchmark displayed in Figure 3 mixes two products: b_1 and b_2, with consecutive concentrations Cb_1 and Cb_2. The flow rates of b_1 and b_2 are w_1 and w_2, respectively. The final obtained product is characterized by three features: the concentration C_b, the flow rate w_0 and the product height h. The interaction between concentration and flow rates is summarized by the following equation system.

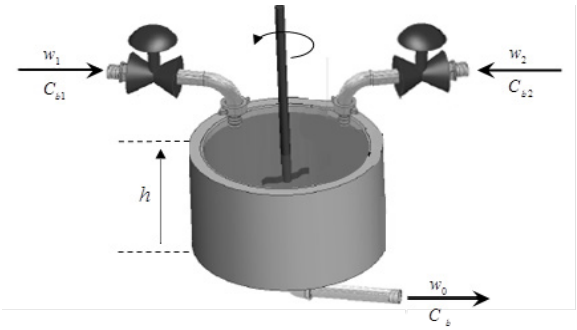

Figure 3. Graph of the CSTR- Benchmark

The physical model of this process is expressed by this following system of nonlinear differential equations:

$$\begin{cases} \dfrac{dh(t)}{dt} = -0,2\sqrt{h(t)} + w_1(t) + w_2(t) \\ \dfrac{dC_b(t)}{dt} = \left(C_{b1} - C_b(t)\right)\dfrac{w_1(t)}{h(t)} - \dfrac{k_1.C_b(t)}{\left(1+k_2.C_b(t)\right)^2} + \left(Cb_{b2} - C_b(t)\right)\dfrac{w_2(t)}{h(t)} \end{cases} \quad (47)$$

In the present case, a subsystem Simple Input Simple Output (SISO) is taken into account, whose input is the flow rate w_1 and whose output is the concentration C_b, as illustrated in Figure 4.

To achieve this, the consumption rates k_1 and k_2, the concentrations C_{b1} and C_{b2} and the flow rate w_2 are assigned to the fixed values given in Table 1.

Table 1. Fixed values of the parameters of the CSTR Benchmark

Parameters	C_{b1}	C_{b2}	w_2	k_1=k_2
Values	25.1 *Kmol.* m^{-3}	0.1 *Kmol.* m^{-3}	$0.7 L.min^{-1}$	0.9

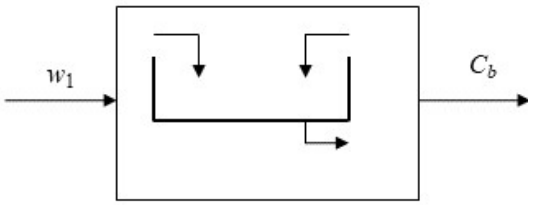

Figure 4. The SISO subsystem of the CSTR Benchmark

For this study, the sampling time is T_e=1s and the system's input w_1 is chosen as a pseudo-random Gaussian signal whose value varies between 0.05

and 2.4 as it can be depicted in Figure 5. The evolution of output signal C_b is plotted in Figure 6.

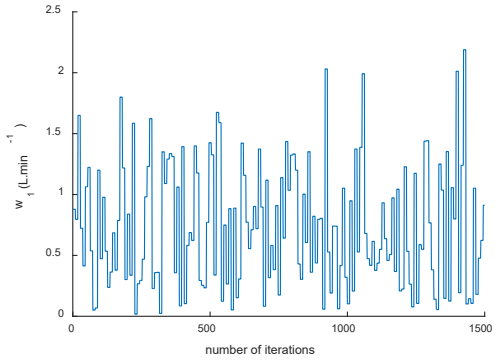

Figure 5. The system's input signal w_1

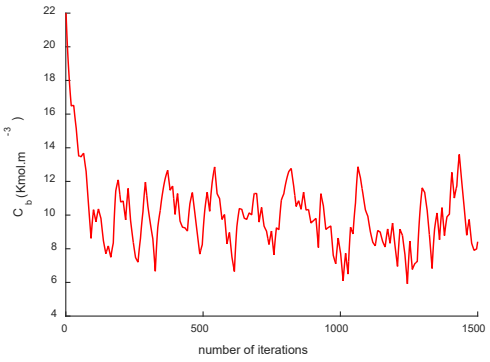

Figure 6. The system's output signal C_b

5.1 Offline Identification of the Parameters

To accomplish the offline identification step, 1000 input/output measurements are used. The yielded model is validated over the remaining 500 measurements.

For the identification phase, Algorithm 1 is employed to identify the Fourier coefficients, the Laguerre poles and the parameters of the weighting functions. The truncating orders values n_a=n_b=2 and the number of submodels is fixed to L=2, in order to reduce the number of parameters that will to be identified. In order to apply Algorithm 1, an initial population of N_{ind}=60 individuals, a crossover rate P_c=90%, a number of generations G_{max}=30, a mutation rate P_m=3.2% and a constant regularization value α=1.2 are taken into consideration. The output of the system is considered as a decision parameter $\zeta(k) = C_b(k)$. So, one obtains two weighting functions $\mu_1(C_b(k))$ and $\mu_2(C_b(k))$ defined by (11), constructed from two Gaussian functions $\omega_1(C_b(k))$ and $\omega_2(C_b(k))$, such that:

$$\omega_s(C_b(k)) = \exp\left(-\frac{(C_b(k)-c_s)^2}{\sigma_s^2}\right), s = 1,2 \quad (48)$$

For the identification phase, the evolution of the parameters of the weighting functions is presented in Figure 7.

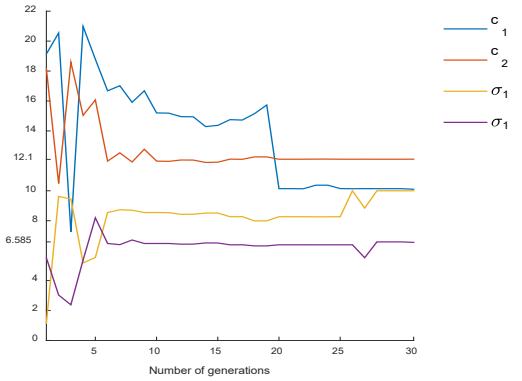

Figure 7. Parameters of weighting functions

The identified weighting functions are plotted in Figures 8.

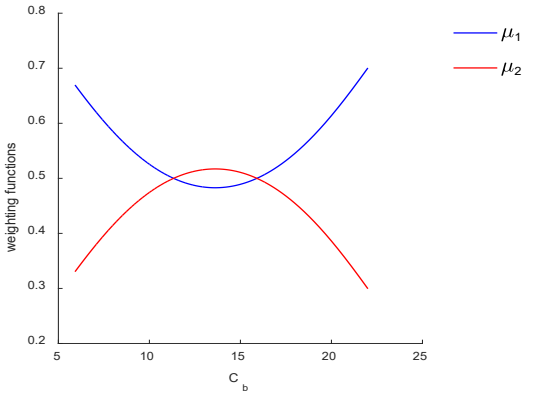

Figure 8. Weighting functions

Figure 9 presents the evolution of the Laguerre poles.

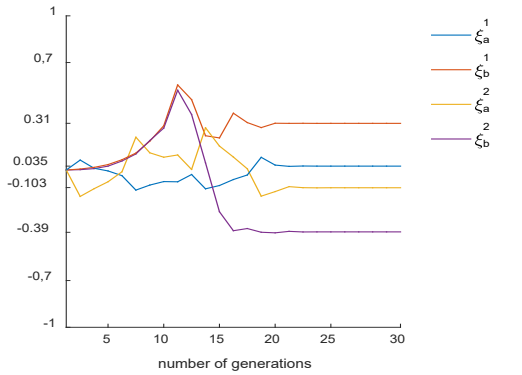

Figure 9. Offline identification of Laguerre poles

The last population (*counter*=30) of parameters of the weighting functions are classified in Table 2 and the Fourier coefficients and optimal Laguerre poles in Table 3, respectively.

Table 2. Identified parameters of the weighting functions

	Values
Gaussian centers	$c = [c_1\ c_2]^T = [10.14\ \ 12.1]^T$
Dispersions	$\sigma = [\sigma_1\ \sigma_2]^T = [10\ \ 6.585]^T$

Table 3. Identified Fourier coefficients and Laguerre poles

s	0	g_{1a}^s	g_{0b}^s
1	0.00013	-0.013	0.7499
2	1. 148	0.01	-0. 48
s	g_{1b}^s	ξ_a^s	ξ_b^s
1	-0.0244	0.035	0.31
2	0.8956	-0.103	-0. 39

The evolution of the *NMSE* of the genetic algorithm is illustrated in Figure 10.

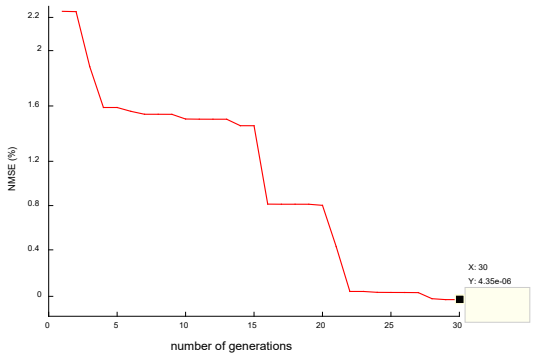

Figure 10. Evolution of the *NMSE*

Over 30 generations, the evaluation function *NMSE* was minimized from one generation to another to converge to a final value of $4.35.10^{-6}$.

The offline recursive estimation of the Fourier coefficients over the offline identification phase is shown in Figure 11. It can be noticed that the identified values converge from iteration 600. Subsequently, Figure 12 illustrates the evolution of the output of the Benchmark $y_m(k) = C_b(k)$ and ARX-Laguerre multimodel output $y_m(k)$ over the validation phase and proves the matching of both outputs.

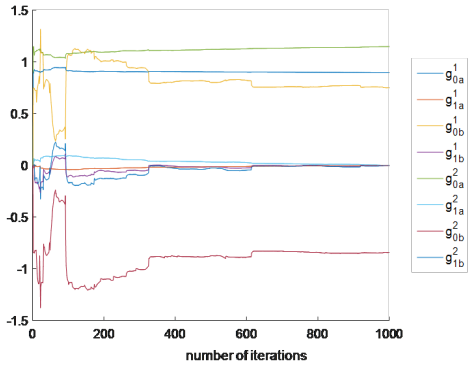

Figure 11. Estimation of Fourier coefficients

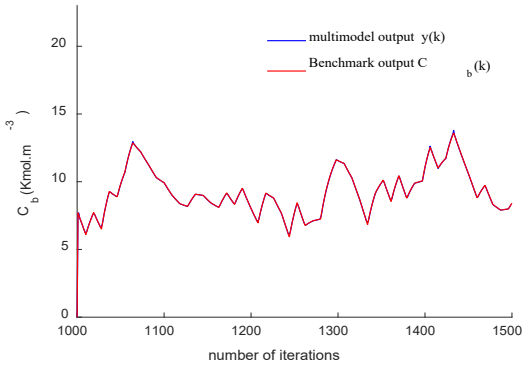

Figure 12. Validation phase of ARX-Laguerre multimodel

5.2 Estimation of the Input Fault of the CSTR Benchmark

Algorithm 2 is applied to carry out this step. The sliding window width is fixed at n_o=*50* and the convergence threshold at $\varepsilon = 10^{-2}$. The weighting functions are calculated based on the values of the parameters in Table 2. Figures 13 and 14 draw the evolution of the estimated fault $\eta_{cal}(k)$ for constant and random fault respectively. In both figures, the estimated values converge to applied ones. By examining these figures, it can be noticed that the new approach of identifying the input fault allows to estimate a random fault with variable and low amplitude.

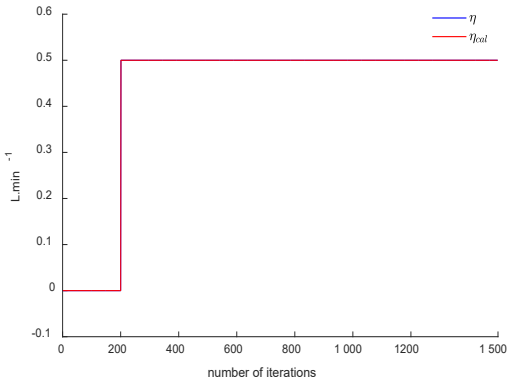

Figure 13. Evolution of the estimated and the constant applied fault

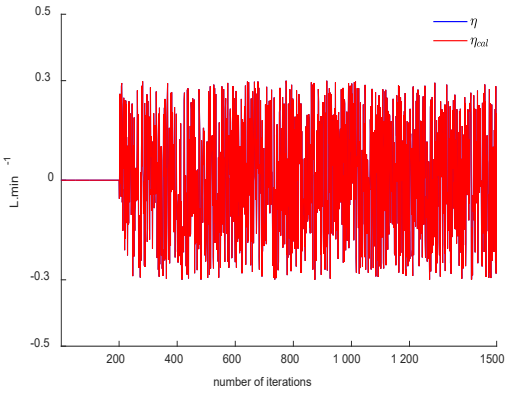

Figure 14. Evolution of the estimated and the random applied fault

The Least Mean Square Errors the real fault and the estimated one for both cases are given by 4.65.10-17 and 1,48.10^{-16} respectively.

The identified Laguerre poles of the ARX-Laguerre multimodel in presence of an input fault for both tests are shown in Figures 15 and 16, respectively.

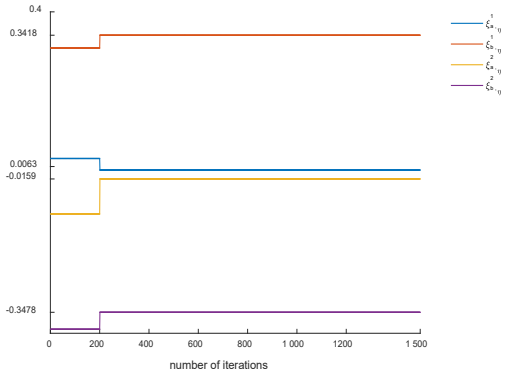

Figure 15. Estimated Laguerre poles in the presence of a constant fault

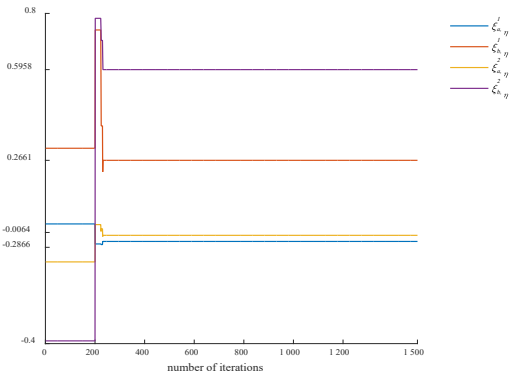

Figure 16. Estimated Laguerre poles in the presence of a random fault

The estimated Fourier coefficients values in Figures 17 and 18.

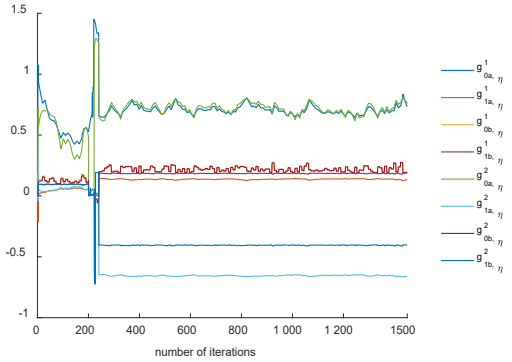

Figure 17. Estimated Fourier coefficients in the presence of a constant fault

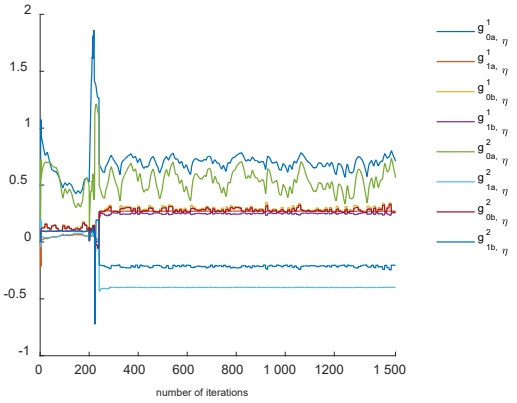

Figure 18. Estimated Fourier coefficients in the presence of a random fault

The evolution of the criterion (46) for both tests is presented in Figures 19 and 20. It can be noticed that this criterion exceeds the threshold value $\varepsilon = 10^{-2}$ at the time of the fault injection. The estimated Laguerre poles and Fourier coefficients are shaken too.

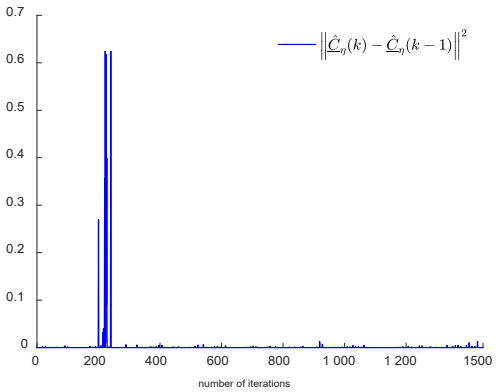

Figure 19. Evolution of the criterion in the presence of a constant fault

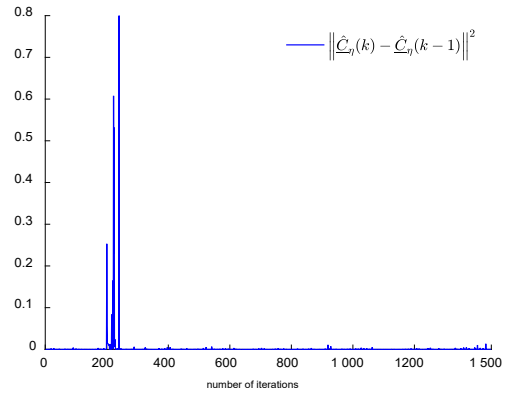

Figure 20. Evolution of the criterion in the presence of a random fault

Figures 21 and 22 draw the output of the ARX-Laguerre multimodel $y_\eta(k)$ and that of the Benchmark $C_b(k)$ in the presence of a fault, at time instant t=200s, for the constant fault and for the variable random fault, respectively.

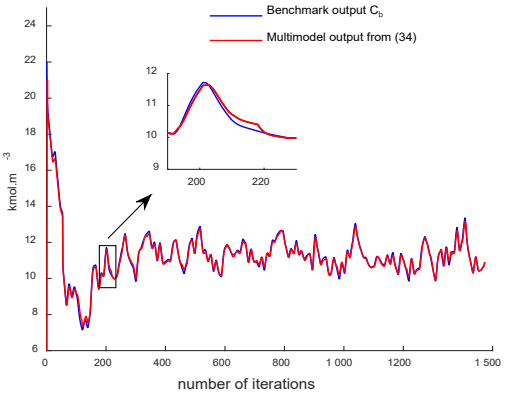

Figure 21. Evolution of $C_b(k)$ and $y_\eta(k)$ case for a constant fault

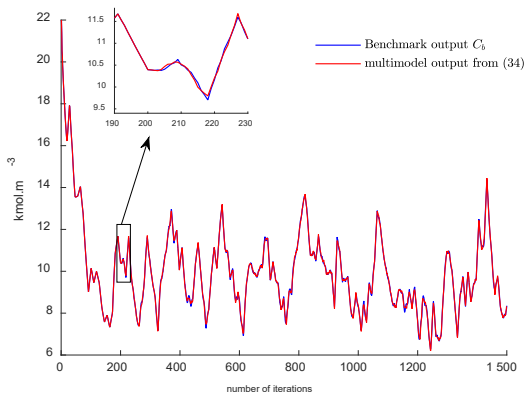

Figure 22. Evolution of $C_b(k)$ and $y_\eta(k)$ case for a random fault

It can be seen that the system output $C_b(k)$ tracks the ARX-Laguerre multimodel output $y_\eta(k)$ for both faults. This observation emphasizes the good performances of the proposed input fault estimation algorithm, as this algorithm is tested for constant and random faults.

To confirm the efficiency of the proposed algorithm, a comparative study with the diagnosis approach using a PI observer based on ARX-Laguerre multimodel was developed (Wang et al., 2023), for the constant and the variable random faults. By fixing β=0.25, one obtains the observer gains K_p and K_I :

$$K_p=\begin{bmatrix}1.0103 & 0.4419 & 0.1006 & 0.2935 & 0.5688 & 0.9868 & 0.1761 & -0.2174\end{bmatrix}^T;\quad K_I=1.6 \tag{49}$$

Figures 23 and 24 show the evolution of the real fault $\eta(k)$ and the estimated one $\hat{\eta}(k)$ for constant and random faults respectively.

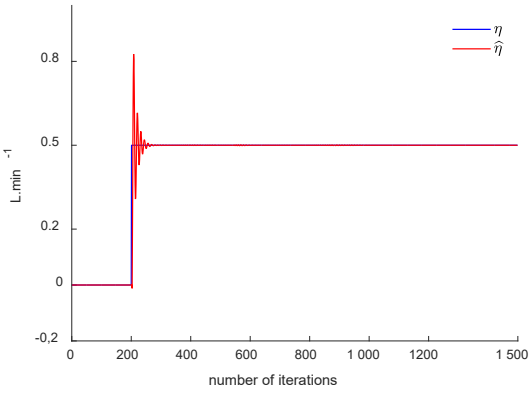

Figure 23. PI observer for test 1 for a constant fault: evolution of $\hat{\eta}(k)$ and $\eta(k)$

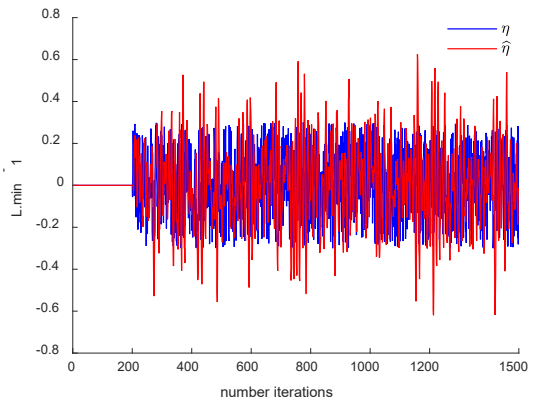

Figure 24. PI observer for test 2 for a variable random fault: evolution of $\hat{\eta}(k)$ and $\eta(k)$

The Benchmark output $C_b(k)$ and the output that was estimated by the PI observer $\hat{y}(k)$ for the case of the constant fault and for the case of the random variable fault are presented in Figures 25 and 26, respectively. We note that the PI observer output

doesn't match the reel system output $C_b(k)$ for constant and random faults which confirms the supremacy of our proposed approach.

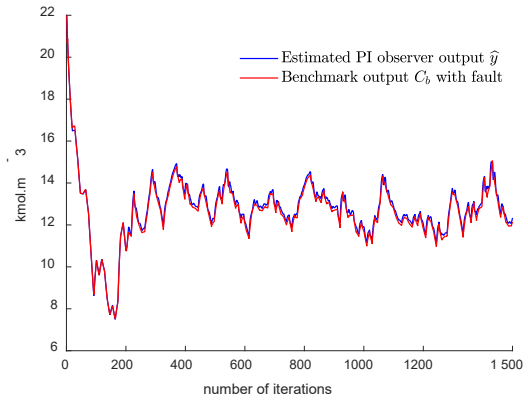

Figure 25. Evolution of $C_b(k)$ and PI observer $\hat{y}(k)$ case for a constant fault

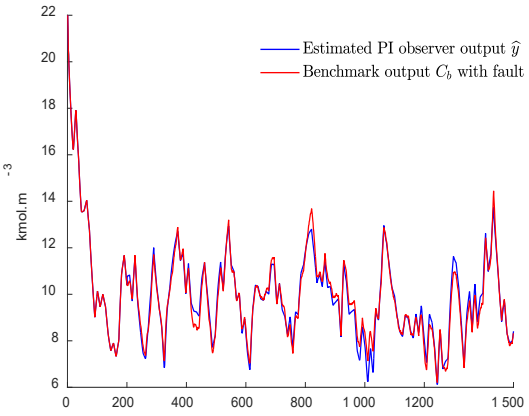

Figure 26. Evolution of $C_b(k)$ and PI observer $\hat{y}(k)$ case for a random fault

6. Conclusion

In this article, a new algorithm for offline parametric identification of the ARX-Laguerre multimodel was developed using genetic algorithms. Subsequently, a new approach for estimating an input fault of a nonlinear SISO system was proposed, based on updating the ARX-Laguerre multimodel parameters over a sliding window. In order to test the effectiveness of the algorithm of the offline identification of the parameters of the ARX-Laguerre multimodel and the proposed approach of input fault estimation, a validation on a CSTR Benchmark was retained with two forms of the fault: constant fault and random variable fault. Finally, a comparative study with another method of fault estimation based on a PI observer was considered. As a future perspective regarding the present work, the exploitation of the fault estimation method should be considered, in order to develop a fault tolerant control which will be able to make use of the nonlinear SISO ARX-Laguerre multimodel.

The suggested input fault estimation method aims to serve as a foundational tool for identifying faults in the system inputs. Subsequently, it will be integrated into the development of a fault-tolerant control that specifically addresses issues arising from actuator faults.

REFERENCES

Adaily, S., Abdelkader, M., Tarek, G. & José, R. (2018) Optimal multimodel representation by Laguerre filters applied to a communicating two tank system. *Journal of Systems Science and Complexity*. 31(3), 621-646. doi: 10.1007/s11424-017-6047-2.

Benamor, H., Njima, C. B., Tarek, G., Abderrahmen, Z. & Hassani, M. (2020) Fault diagnosis based on ARX-Laguerre multimodel. In: *2020 International Conference on Control, Automation and Diagnosis (ICCAD), 07-09 October 2020, Paris, France*. pp. 1-6. doi: 10.1109/ICCAD49821.2020.9260522.

Bouzrara, K., Garna, T., Ragot, J. & Messaoud, H. (2013) Online identification of the ARX model expansion on Laguerre orthonormal bases with filters on model input and output. *International Journal of Control*. 86(3), 369-385. doi: 10.1080/00207179.2012.732710.

Brouri, A., Kadi, L. & Lahdachi, K. (2022) Identification of nonlinear system composed of parallel coupling of Wiener and Hammerstein models. *Asian Journal of Control*. 24(3), 1152-1164. doi: 10.1002/asjc.2533.

Fang, P., Fu, W., Wang, K., Xiong, D. & Zhang, K. (2022) A compositive architecture coupling outlier correction, EWT, nonlinear Volterra multi-model fusion with multi-objective optimization for short-term wind speed forecasting. *Applied Energy*. 307, 118-191. doi: 10.1016/j.apenergy.2021.118191.

Han, J., Liu, X., Wei, X. & Hu, X. (2023) Adaptive adjustable dimension observer based fault estimation for switched fuzzy systems with unmeasurable premise variables. *Fuzzy Sets and Systems*. 452, 149-167. doi: 10.1016/j.fss.2022.06.017.

Levin, D., Bastos, K. K. & Dowell, E. H. (2022) Convolution and Volterra series approach to reduced-order modeling of unsteady aerodynamic loads. *American Institute of Aeronautics and Astronautics (AIAA) Journal*. 60(3), 1663-1678. doi: 10.2514/1.J060391.

Li, Y., Xu, W. & Chang, L. (2023) Fuzzy model based fault estimation and fault tolerant control for flexible spacecraft with unmeasurable vibration modes. *IET Control Theory & Applications*. 17(1), 19-38. doi: 10.1049/cth2.12357.

Mzyk, G. & Wachel, P. (2017) Kernel-based identification of Wiener–Hammerstein system. *Automatica*. 83, 275-281. doi: 10.1016/j.automatica.2017.06.038.

Nguyen, D. H. & Yin, G. (2017) Coexistence and exclusion of stochastic competitive Lotka–Volterra models. *Journal of Differential Equations*. 262(3), 1192-1225. doi: 10.1016/j.jde.2016.10.005.

Quachio, R. & Garcia, C. (2019) MPC relevant identification method for Hammerstein and Wiener models. *Journal of Process Control*. 80, 78-88. doi: 10.1016/j.jprocont.2019.01.011.

Seborg, D. E., Edger, T. E. & Millichamp, D. A. (2004) *Process Dynamics and Control*. 2nd ed. New Jersey, SUA, John Wiley & Sons.

Shin, Y. E., Sohn, S. D., Han, H., Park, Y., Shin, H. J. & Ko, H. (2020) Self-powered triboelectric/pyroelectric multimodal sensors with enhanced performances and decoupled multiple stimuli. *Nano Energy*. 72, 104671. doi: 10.1016/j.nanoen.2020.104671.

Takagi, T. & Sugeno, M. (1985) Fuzzy identification of systems and its applications to modeling and control. *IEEE Transactions on Systems, Man, and Cybernetics*. SMC-15(1), 116-132. doi: 10.1109/TSMC.1985.6313399.

Vajda, P, Eiben, A. E & Hordijk, W. (2008) Parameters control methods for selection operators in genetic algorithms. In: Rudolph, G., Jansen, T., Beume, N., Lucas, S., Poloni, C. (eds.) *Parallel Problem Solving from Nature-PPSN X*. Lecture note in Computer Science, vol 5199. Berlin, Heidelberg, Springer, pp. 620-630.

Wang, X. (2020) *Machine learning approach for high speed link modeling and IBIS-AMI model generation*. Dissertation. University of Illinois at Urbana-Champaign.

Wang, Y., Hao, L. Y., Li, T. & Chen, C. P. (2023) Integral sliding mode-based fault-tolerant control for dynamic positioning of unmanned marine vehicles based on a TS fuzzy model. *Journal of Marine Science and Engineering*. 11(2), 370. doi: 10.3390/jmse11020370.

Wang, Y., Tang, S. & Gu, X. (2022) Parameter estimation for nonlinear Volterra systems by using the multi-innovation identification theory and tensor decomposition. *Journal of the Franklin Institute*. 359(2), 1782-1802. doi: 10.1016/j.jfranklin.2021.11.015.

Young, C. & Holsteen, K. (2017) Model uncertainty and robustness: A computational framework for multimodel analysis. *Sociological Methods & Research*. 46(1), 3-40. doi: 10.1177/0049124115610347.

Zhang, X., Zhang, J. X., Huang, W. & Shi, P. (2023) Non-fragile sliding mode observer based fault estimation for interval type-2 fuzzy singular fractional order systems. *International Journal of Systems Science*. 54(7), 1451-1470. doi: 10.1080/00207721.2023.2177904.